

Paper No. : DY 13  
**A General Structural Model for Thin- and Thick-Walled  
Composite Blades with Elastic Couplings**

Sung Nam Jung\*      V. T. Nagaraj†      Inderjit Chopra‡

*Alfred Gessow Rotorcraft Center  
Department of Aerospace Engineering  
University of Maryland, College Park, MD 20742, USA*

A general structural model, which is an extension of the Vlasov theory, is proposed for the analysis of composite rotor blades with elastic couplings. A comprehensive analysis applicable to both thick- and thin-walled composite beams, which can have either open- or closed profiles is formulated. The theory accounts for the effects of elastic couplings, shell wall thickness, and transverse shear deformations. A semi-complementary energy functional is used to account for the shear stress distribution in the shell-wall. The bending and torsion related warpings and the shear correction factors are obtained in closed form as part of the analysis. The resulting first order shear deformation theory (Timoshenko) describes the beam kinematics in terms of the axial, flap and lag bending, flap and lag shear, torsion and torsion-warping deformations. As examples, the stiffness coefficients for bending-torsion and extension-torsion coupled I-beams are presented. The theory is validated against experimental results for I-beams with elastic couplings.

## 1. Introduction

During the past two decades, advanced composites are finding increasing applications in the construction of helicopter rotor blades. At the present time, there is a good understanding of the design and manufacturing practices of composite rotor blades, but the analytical tools are not fully developed in particular for structurally tailored composite rotors. The favorable properties of fiber reinforced composites, such as higher specific strength and stiffness, superior damage tolerance and capability for manufacturing more complex

geometries than metals, make them attractive for rotorcraft applications. Existing blade designs incorporate balanced composite laminates in which structural couplings are designed to be zero. It is now well established that composites offer the potential of certain structural couplings that can have a favorable influence on the aeroelastic behavior of rotor blades to improve performance, increase aero-mechanical stability and minimize vibration and blade loads. Such couplings have not been exploited in current rotor designs partly because of the non-availability of

---

\* Visiting Assistant Professor, Chonbuk National University, Korea

† Senior Research Scientist

‡ Minta-Martin Professor, Director

proven analytical methods for accurately predicting the response of such blades.

Composite rotor blades are normally of closed single- or multi-celled cross-sections and are thin-walled except near the root where they become thick walled. The flex-beams of bearingless rotors are often of open cross-section such as solid rectangular, I-section, or cruciform-section beams. Apart from the possibility of using different materials such as glass, graphite and kevlar, various lay-up schemes can be used for the construction of the rotor blades to improve their performance.

During the past decade, there has been a phenomenal growth of research activities to develop methodology to analyze composite tailored rotor blades. These range from simple analytical models to detailed finite element methods. These methods have been validated using other analyses and experimental data from simple specimens and sometimes from scale models. These studies have led to a better understanding of the structural behavior of composite rotor blades and to the importance of nonclassical effects such as out-of-plane warping, warping restraint, and transverse shear on the behavior of composite blades. Jung *et al.* [1] made an assessment of the current techniques of modeling composite rotor blades and identified, among others, the need for a Timoshenko type model which will take into account such features as elastic couplings, thickness of the shell wall and that will be applicable to beams having open- or closed cross-sections. Such a model should also be capable of modeling cross-section warping due to bending and torsion.

Common to both thin-walled and thick-walled blade analysis is the need to properly model the local behavior of the shell wall as a reaction to the global deformation of the blade. The wall behaves as a thin- or thick-walled shell and undergoes both in-plane and out-of-plane deformations (warpings) in

response to the applied external loading. It is important to model these warpings consistently in order to obtain accurate results for the beam response [1].

The modeling of rotor blades can be formulated through either a displacement or a force method. The displacement formulation, also called the stiffness formulation has been used, among others, by Rehfield and co-workers [2, 3], Smith and Chopra [4], Chandra and Chopra [5]. This formulation is based on suitable approximations to the displacement field of the shell wall. The assumed displacement field is used to compute the strain energy, and using the energy principles yields the beam stiffness relations as well as equations of motion. In displacement based models, the distribution of warping across the cross-section can only be applied to simple cross-sections. There is no systematic method to decide on the distribution of the warping distribution to a generic section and the choice of suitable functions for such cases is a matter of individual judgement. For example, the torsion related warping is assumed to be the same as that for an isotropic beam by Rehfield [2]; this has been modified to include the variable shear modulus by Chandra and Chopra [5]. The warping related with the transverse shear is not modeled in the above references. Also, in the displacement modes of these methods do not satisfy the equations of equilibrium of the shell wall and lead to overestimates of the beam stiffnesses.

In the force formulation, also called the flexibility formulation, the direct stress in the shell wall is assumed and the distribution of the shear stress and the related warpings are obtained from the equilibrium equations of the shell wall. The flexibility method provides a systematic method of choosing the warping functions. This method has been used by Mansfield and Sobey [6] and Libove [7] and more recently by Johnson *et al.* [8] for thin walled composite blades with closed profiles.

While these methods give a better representation of the shear stresses, and hence a better accuracy, they have not found wide application since most of the comprehensive analysis codes use the displacement method.

Berdichevsky *et al.* [9] and Suresh and Nagaraj [10] used the displacement method along with the shear-related warping functions derived from the equations of equilibrium. Berdichevsky and co-workers used the variational-asymptotic approach in which the shear related terms are refined in an iterative manner from an assumed direct strain terms in conjunction with the equations of equilibrium of an element of the shell wall. In the shear-related deformations, terms which contribute below a certain level to the strain energy are neglected. They have applied their method (which is equivalent to an Euler-Bernoulli model) to analyze thin-walled composite beams of both open- and closed cross-sections. Ref. 10 also used the equilibrium equations of the shell wall to generate the shear-related terms from an assumed axial deformation. They retained all the terms in the shear related deformation and have examined the shear lag phenomenon in thin-walled composite beams with closed cross-sections. Hodges *et al.* [11] used the variational asymptotic method to derive the asymptotically correct stiffness matrix and warping displacements for a general, nonhomogeneous and anisotropic beam cross-sections. The elements of stiffness matrix were developed using a finite element technique.

In the present paper, a comprehensive analysis applicable to both thick- and thin-walled composite beams, which can have either open- or closed profile is presented. The theory accounts for the effects of elastic couplings, shell wall thickness, and transverse shear deformations. The shear related terms are obtained from the equations of equilibrium of the shell wall and higher order terms are not discarded. A

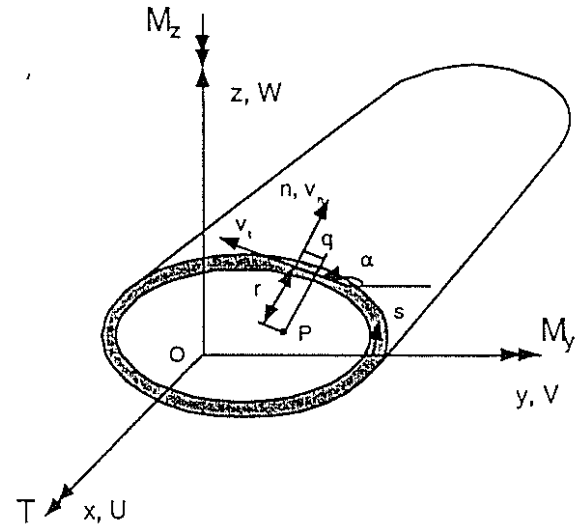


Fig. 1 Coordinate systems and deformations.

semi-complementary energy functional is used to satisfy, in a variationally consistent manner, the continuity condition for displacements and transverse stresses. The bending and torsion related warpings are obtained in closed form as part of the analysis and lead to the shear correction factors. The resulting first order (Timoshenko) shear deformation theory describes the beam kinematics in terms of the axial, flap and lag bending, flap and lag shear, torsion and torsion-warping deformations.

## 2. Theoretical Formulation

Figure 1 shows the geometry and coordinate systems for composite blades with arbitrary cross sections. Two coordinate systems are introduced in the present formulation: an orthogonal Cartesian coordinate system  $(x, y, z)$  for the beam, where  $x$  is the reference axis of the beam and  $y$  and  $z$  are the transverse coordinates of the cross section; a curvilinear coordinate system  $(x, s, n)$  for the shell wall of the section, where  $s$  is a contour coordinate and is measured along the tangent to the middle surface of the shell wall, and  $n$  is normal to this contour coordinate.

### 2.1 Fundamental Assumptions

The following assumptions are made in the present theory:

- 1) The contour of a cross section does not deform in its own plane. This means that the inplane warping of the cross section is neglected and the zero inplane strain assumption ( $\epsilon_{ss}$  and  $\kappa_{ss}$ ) or zero inplane stress assumption ( $N_{ss}$  and  $M_{ss}$ ) is used for the constitutive relations. This assumption is made to relate the position vectors of a point on the beam cross-section before and after deformation in a unique way.
- 2) Kirchhoff assumption, which states that the straight lines remain straight during a deformation, holds for the shell wall.

## 2.2 Kinematics

The global deformations of the beam are ( $U$ ,  $V$ ,  $W$ ) along the  $x$ ,  $y$  and  $z$  axes, and  $\phi$  denotes the twist about the  $x$ -axis. The local shell deformations are ( $u$ ,  $v_s$ ,  $v_n$ ) along the  $x$ ,  $s$  and  $n$  directions, respectively. From the geometric considerations (Fig. 1) and the assumption 1 made in the previous section, the shell displacements  $v_n$  and  $v_s$  are related to the beam displacements  $V$ ,  $W$  and  $\phi$  as:

$$\begin{aligned} v_t &= V y_{,s} + W z_{,s} + r\phi \\ v_n &= V z_{,s} - W y_{,s} - q\phi \end{aligned} \quad (2.1)$$

where  $r$  and  $q$  are shown in Fig. 1 and have the relation:

$$\begin{aligned} r &= y \sin \alpha - z \cos \alpha = y z_{,s} - z y_{,s} \\ q &= y \cos \alpha + z \sin \alpha = y y_{,s} + z z_{,s} \end{aligned} \quad (2.2)$$

where  $\alpha$  is defined in Fig. 1. Assuming that the Kirchhoff-Love hypothesis is valid, the displacements of a point on the shell wall away from the mid-plane are given by [12]:

$$\begin{aligned} u &= u^0 - n v_{n,x} \\ v_n &= v_n^0 \\ v_t &= v_t^0 - n \left( v_{n,s}^0 - \frac{v_t^0}{a} \right) \end{aligned} \quad (2.3)$$

where  $a$  is the radius of curvature and  $u^0$ ,  $v_n^0$  and  $v_t^0$  are displacements at the mid-plane. The strain-displacement relations for the shell wall are [12]:

$$\begin{aligned} \left[ \epsilon_{xx} \quad \epsilon_{ss} \quad \gamma_{xs} \right]^T &= \left[ u_{,x}^0 \quad v_{t,s}^0 + \frac{v_n^0}{a} \quad u_{,x}^0 + v_{t,x}^0 \right]^T \\ \gamma_{xn} &= \gamma_{xy} z_{,s} - \gamma_{xz} y_{,s} \\ \left\{ \begin{array}{l} \kappa_{xx} \\ \kappa_{ss} \\ \kappa_{xs} \end{array} \right\} &= \left\{ \begin{array}{l} -v_{n,xx}^0 + \gamma_{xn,x} \\ -(v_{n,s}^0 + \frac{v_t^0}{a})_{,s} \\ (\frac{v_t^0}{a})_{,x} - 2v_{n,xx}^0 \end{array} \right\} \end{aligned} \quad (2.4)$$

Equations (2.3) and (2.4) are based on the geometry of a cylindrical shell of any general cross section. Hence no assumption of flat plate is made. The term  $\gamma_{xn}$  is included to represent the transverse shear strains in the wall. Inserting the compatibility condition of the section (Eq. (2.1)) into Eq. (2.4), the strains in the shell wall are obtained as:

$$\begin{aligned} \epsilon_{xx} &= u_{,x}^0 \\ \gamma_{xs} &= u_{,s}^0 + V_{,x} y_{,s} + W_{,x} z_{,s} + r\phi_{,x} \\ \kappa_{xx} &= \beta_{z,x} z_{,s} - \beta_{y,x} y_{,s} + q\phi_{,xx} \\ \kappa_{xs} &= -2\phi_{,x} \\ \epsilon_{ss} &= 0 = \kappa_{ss} \end{aligned} \quad (2.5)$$

where  $\beta_y$  and  $\beta_z$  are cross section rotations about the  $y$  and  $z$  axes, respectively and is given by the relation as:

$$\begin{aligned} \beta_y &= \gamma_{xz} - W_{,x} \\ \beta_z &= \gamma_{xy} - V_{,x} \end{aligned} \quad (2.6)$$

In Eq. (2.5), the axial displacement  $u$  has not been specified. This consists of the

following: (a) axial displacement of the beam; (b) axial warping due to bending; (c) axial warping due to torsion; (d) axial warping due to transverse shear; and (e) axial warping due to higher order transverse shear effects. To obtain a first approximation to  $u$ , we use the definition of shear strain. In terms of the component strains, the shear strain  $\gamma_{xs}$  is:

$$\gamma_{xs} = \gamma_{xy}y_{,s} + \gamma_{xz}z_{,s} \quad (2.7)$$

In terms of the displacements, the shear strain is also given by:

$$\gamma_{xs} = u_{,s}^0 + v_{,x}^0 = u_{,s}^0 + V_{,x}y_{,s} + W_{,x}z_{,s} + r\phi_{,x} \quad (2.8)$$

Equating Eqs. (2.7) and (2.8), and integrating from 0 to  $s$ , we obtain the first approximation for  $u$  as:

$$u^0 = U + y\beta_z + z\beta_y - \omega\phi_{,x} \quad (2.9)$$

where the sectorial area  $\omega$  is defined as:

$$\omega = \int_0^s r ds \quad (2.9a)$$

Using the relation in Eq. (2.9), the strain-displacement relations in Eq. (2.5) can be written as:

$$\begin{aligned} \epsilon_{xx} &= U_{,x} + z\beta_{y,x} + y\beta_{z,x} - \bar{\omega}\phi_{,xx} \\ \kappa_{xx} &= z_{,s}\beta_{z,x} - y_{,s}\beta_{y,x} + q\phi_{,xx} \\ \kappa_{xs} &= -2\phi_{,xs} \\ \gamma_{xs} &= u_{,s}^0 + V_{,x}y_{,s} + W_{,x}z_{,s} + r\phi_{,x} \\ \gamma_{xn} &= u_{,n}^0 + V_{,x}z_{,s} - W_{,x}y_{,s} - q\phi_{,x} \end{aligned} \quad (2.10)$$

### 2.3 Constitutive Relations

The constitutive relations between the stress resultants and the strains are given by

$$\begin{Bmatrix} N_{xx} \\ N_{xs} \\ M_{xx} \\ M_{xs} \end{Bmatrix} = \begin{bmatrix} A_{11} & A_{16} & B_{11} & B_{16} \\ A_{16} & A_{66} & B_{16} & B_{66} \\ B_{11} & B_{16} & D_{11} & D_{16} \\ B_{16} & B_{66} & D_{16} & D_{66} \end{bmatrix} \begin{Bmatrix} \epsilon_{xx} \\ \gamma_{xs} \\ \kappa_{xx} \\ \kappa_{xs} \end{Bmatrix} \quad (2.11)$$

where,  $A_{ij}$ ,  $B_{ij}$  and  $D_{ij}$  are laminate stiffnesses for extension, extension-bending coupling and bending, respectively [13]. These stiffness components are obtained using zero inplane strain assumption. When zero inplane stress assumption is used, the stiffness components are to be adjusted in an appropriate manner. The above constitutive relations can be rewritten in a semi-inverted form as:

$$\begin{Bmatrix} N_{xx} \\ M_{xx} \\ M_{xs} \\ \gamma_{xs} \end{Bmatrix} = \begin{bmatrix} A_{n\epsilon} & A_{n\kappa} & A_{n\phi} & A_{n\tau} \\ A_{n\kappa} & A_{m\kappa} & A_{m\phi} & A_{m\tau} \\ A_{n\phi} & A_{m\phi} & A_{\phi\phi} & A_{\phi\tau} \\ -A_{n\tau} & -A_{m\tau} & -A_{\phi\tau} & A_{\gamma\tau} \end{bmatrix} \begin{Bmatrix} \epsilon_{xx} \\ \kappa_{xx} \\ \kappa_{xs} \\ N_{xs} \end{Bmatrix}$$

$$Q_n = A_{xn}\gamma_{xs} \quad (2.12)$$

where  $Q_n$  is the transverse shear force in the wall and the respective stiffness components in Eq. (2.12) have the relation:

$$\begin{aligned} A_{n\epsilon} &= (A_{11} - \frac{A_{16}^2}{A_{66}}) \quad , \quad A_{n\kappa} = (B_{11} - \frac{A_{16}B_{16}}{A_{66}}) \\ A_{n\phi} &= (B_{16} - \frac{A_{16}B_{66}}{A_{66}}) \quad , \quad A_{\phi\phi} = (D_{66} - \frac{B_{66}^2}{A_{66}}) \\ A_{m\kappa} &= (D_{11} - \frac{B_{16}^2}{A_{66}}) \quad , \quad A_{m\phi} = (D_{16} - \frac{B_{16}B_{66}}{A_{66}}) \\ A_{\gamma\tau} &= \frac{1}{A_{66}} \quad , \quad A_{\phi\tau} = \frac{B_{66}}{A_{66}} \quad , \quad A_{n\tau} = \frac{A_{16}}{A_{66}} \quad , \quad A_{m\tau} = \frac{B_{16}}{A_{66}} \end{aligned} \quad (2.13)$$

### 2.4 Derivation of the Equations of Motion

Based on the above kinematic and constitutive relations, we obtain the governing equations for the beam. Introducing the semi-complementary energy function  $\Phi_c$  which was proposed by

Murakami *et al.* [14], the variational statement for the beam gives

$$\int_0^L \int_C \delta \{ \Phi_c(\varepsilon_{xx}, \kappa_{xx}, \kappa_{xs}, \gamma_{xs}, N_{xs}) + \gamma_{xs}^c N_{xs} \} ds dx - \delta W_0 = 0 \quad (2.14)$$

where  $L$  is the length of the beam,  $\delta W_0$  is the virtual work of the external forces and moments, and the first variation of the energy functional  $\delta \Phi_c$  is given by:

$$\delta \Phi_c = \frac{1}{2} \{ N_{xx} \delta \varepsilon_{xx} + M_{xx} \delta \kappa_{xx} + M_{xs} \delta \kappa_{xs} + Q_n \delta \gamma_{xs} - \gamma_{xs}^k N_{xs} \} \quad (2.14a)$$

Note that  $\gamma_{xs}^c$  and  $\gamma_{xs}^k$  in Eq. (2.14) are used here for convenience and the superscript  $c$  and  $k$  stand for constitutive and kinematics, respectively, and denote the origins of the strain quantities.

### Determination of $N_{xs}$

In order to evaluate each of energy terms in the variational equation in Eq. (2.14), we have to determine the reactive force component  $N_{xs}$  in terms of known quantities. The other terms in Eq. (2.14) can be obtained from the constitutive relations (Eq. (2.11)) and the strain-displacement relations (Eq. (2.10)). For this goal, we use the equilibrium equations of an element of the shell wall, which can be written as:

$$\begin{aligned} N_{xx,x} + N_{xs,s} &= 0 \\ N_{xs,x} &= 0 \end{aligned} \quad (2.15)$$

The second equation in Eq. (2.14) states that  $N_{xs}$  is a function of only  $s$ . Combining this equation with Eq. (2.10) gives

$$\begin{aligned} N_{xs,x} &= 0 \\ &= A_{16} \varepsilon_{xx,x} + A_{66} \gamma_{xs,x} + B_{16} \kappa_{xx,x} + B_{66} \kappa_{xs,x} \end{aligned} \quad (2.16)$$

and we get the relation:

$$\gamma_{xs,x} = -\frac{A_{16}}{A_{66}} \varepsilon_{xx,x} - \frac{B_{16}}{A_{66}} \kappa_{xx,x} - \frac{B_{66}}{A_{66}} \kappa_{xs,x} \quad (2.16a)$$

Using the equations (2.10) and (2.16a) and taking the integration with  $s$ ,

$$\begin{aligned} N_{xs} &= N_{xs}^0 - \int_0^s N_{xs,x} ds \\ &= N_{xs}^0 - \int_0^s \{ (A_{11} - \frac{A_{16}^2}{A_{66}}) \varepsilon_{xx,x} + (B_{11} - \frac{A_{16} B_{16}}{A_{66}}) \kappa_{xx,x} + (B_{16} - \frac{A_{16} B_{66}}{A_{66}}) \kappa_{xs,x} \} ds \\ &= N_{xs}^0 - \int_0^s \{ A_{n\varepsilon} \varepsilon_{xx,x} + A_{n\kappa} \kappa_{xx,x} + A_{n\phi} \kappa_{xs,x} \} ds \end{aligned} \quad (2.17)$$

where  $N_{xs}^0$  is an integration constant (constant shear flow) and is zero for open section beams. Using the strain-displacement relations for  $\varepsilon_{xx}$ ,  $\kappa_{xx}$  and  $\kappa_{xs}$ , Eq. (2.17) leads to:

$$\begin{aligned} N_{xs} &= N_{xs}^0 - S_x U_{,xx} - S_y \beta_{z,xx} - S_z \beta_{y,xx} \\ &\quad - S_\omega \phi_{,xxx} + S_\phi \phi_{,xx} \end{aligned} \quad (2.18)$$

with

$$\begin{aligned} S_x &= \int_0^s A_{n\varepsilon} ds \\ S_y &= \int_0^s (A_{n\varepsilon} y + A_{n\kappa} z_{,s}) ds \\ S_z &= \int_0^s (A_{n\varepsilon} z - A_{n\kappa} y_{,s}) ds \\ S_\omega &= \int_0^s (-A_{n\varepsilon} \bar{\omega} + A_{n\kappa} q) ds \\ S_\phi &= \int_0^s 2A_{n\phi} ds \end{aligned} \quad (2.18a)$$

For closed cross-section beams,  $N_{xs}^0$  is obtained using the continuity condition, which is  $\oint u_{,s} ds = 0$ . From the constitutive equation of Eq. (2.11), the shear strain  $\gamma_{xs}^c$  can be written as:

$$\gamma_{xx}^c = -A_{nr}\epsilon_{xx} - A_{mr}K_{xx} - A_{\phi r}K_{xx} + A_{\gamma r}N_{xx} \quad (2.19)$$

From the strain-displacement relations, we have:

$$\gamma_{xx}^k = u_{,s} + V_{,x}y_{,s} + W_{,x}z_{,s} + r\phi_{,x} \quad (2.20)$$

Equating Equations (2.19) and (2.20), and using the continuity condition for the section, we obtain the shear flow equation as:

$$\begin{aligned} N_{xx}^0 = \frac{1}{\oint A_{\gamma r} ds} & [2A_0\phi_{,x} + \oint A_{nr}\epsilon_{xx} ds + \oint A_{mr}K_{xx} ds \\ & + \oint A_{\phi r}K_{xx} ds + U_{,xx}\oint A_{\gamma r}S_x ds + \beta_{z,xx}\oint A_{\gamma r}S_y ds \\ & + \beta_{y,xx}\oint A_{\gamma r}S_z ds + \phi_{,xxx}\oint A_{\gamma r}S_\omega ds - \phi_{,xx}\oint A_{\gamma r}S_\phi ds] \end{aligned} \quad (2.21)$$

where  $A_0$  is the enclosed area of the cross section. Substituting Eq. (2.21) into Eq. (2.18) and simplifying this equation leads to:

$$\begin{aligned} N_{xx} = f_x U_{,x} + f_y \beta_{z,x} + f_z \beta_{y,x} + f_\omega \phi_{,xx} + f_\phi \phi_{,x} \\ + F_x U_{,xx} + F_y \beta_{z,xx} + F_z \beta_{y,xx} + F_\omega \phi_{,xxx} + F_\phi \phi_{,xx} \end{aligned} \quad (2.22)$$

where,

$$\begin{aligned} f_x = \frac{\oint A_{nr} ds}{\oint A_{\gamma r} ds}, \quad f_y = \frac{\oint A_{nr} y ds + \oint A_{mr} z_{,s} ds}{\oint A_{\gamma r} ds} \\ f_z = \frac{\oint A_{nr} z ds - \oint A_{mr} y_{,s} ds}{\oint A_{\gamma r} ds} \\ f_\omega = \frac{-\oint A_{nr} \bar{\omega} ds + \oint A_{mr} q ds}{\oint A_{\gamma r} ds} \\ f_\phi = \frac{2A_0 - 2\oint A_{\phi r} ds}{\oint A_{\gamma r} ds} \end{aligned} \quad (2.22a)$$

$$F_x = \frac{\oint A_{\gamma r} S_x ds}{\oint A_{\gamma r} ds} - S_x, \quad F_y = \frac{\oint A_{\gamma r} S_y ds}{\oint A_{\gamma r} ds} - S_y$$

$$F_z = \frac{\oint A_{\gamma r} S_z ds}{\oint A_{\gamma r} ds} - S_z, \quad F_\omega = \frac{\oint A_{\gamma r} S_\omega ds}{\oint A_{\gamma r} ds} - S_\omega$$

$$F_\phi = \frac{-\oint A_{\gamma r} S_\phi ds}{\oint A_{\gamma r} ds} + S_\phi$$

For open cross-section beams, the following modifications are needed:

$$f_i = 0 \quad \text{for } i = (x, y, z, \omega, \phi)$$

$$F_i = -S_i \quad \text{for } i = (x, y, z, \omega) \quad \text{and} \quad F_\phi = S_\phi \quad (2.23)$$

Using the notation of Gjelsvik [15], the shear flow equation of  $N_{xx}$  can be written in a symbolic form as:

$$N_{xx} = N_{xx}^a + N_{xx}^r \quad (2.24)$$

where the superscript  $a$  and  $r$  denote active and reactive forces, respectively. The first derivative terms in Eq. (2.22) are active shear components and the second derivative terms are reactive components.

Inserting the equations (2.19) and (2.20) into the variation equations in Eq. (2.14), we can identify the cross-section stress resultants as:

$$\begin{aligned} N &= \int_C N_{xx} ds \\ M_y &= \int_C [N_{xx} z - M_{xx} y_{,s}] ds \\ M_z &= \int_C [N_{xx} y + M_{xx} z_{,s}] ds \\ M_\omega &= \int_C [-N_{xx} \bar{\omega} + M_{xx} q] ds \\ T_s &= \int_C [-N_{xx}^a (r - \bar{\omega}_{,s}) - 2M_{xx}] ds \\ V_y &= \int_C [(N_{xx}^a + N_{xx}^r) y_{,s} + Q_n z_{,s}] ds \\ V_z &= \int_C [(N_{xx}^a + N_{xx}^r) z_{,s} - Q_n y_{,s}] ds \end{aligned} \quad (2.25)$$

where  $T_s$  is St. Venant torsion and  $V_y$  and  $V_z$  are shear loads acting in the  $y$  and  $z$  coordinates, respectively. In obtaining Eq.

(2.25), we use the following relation that can be readily proved:

$$\int_C (\gamma_{xx}^k - \gamma_{xx}^e) ds = 0 \quad (2.26)$$

Using the relations (2.10), (2.12) and (2.22) with application of the calculus of variations, the Eq. (2.25) can be expanded as:

$$\{\bar{\mathbf{F}}_b\} = [\mathbf{C}]\{\bar{\mathbf{q}}_b\} + [\bar{\mathbf{B}}]\{\bar{\mathbf{q}}_{b,x}\} \quad (2.27)$$

where,

$$\begin{aligned} [\bar{\mathbf{F}}_b]^T &= [N \ M_z \ M_y \ M_\omega \ T_x]^T \\ [\bar{\mathbf{q}}_b]^T &= [U_{,x} \ \beta_{z,x} \ \beta_{y,x} \ \phi_{,xx} \ \phi_{,x}]^T \end{aligned} \quad (2.27a)$$

In Eq. (2.27), the components in  $[\mathbf{C}]$  matrix are given in Appendix (a.1). The first term on the right hand side of Eq. (2.27) represents the contribution of the active forces and the second term that of the reactive forces. The elements of the matrix  $[\bar{\mathbf{B}}]$  can be obtained using the definition of  $N_{xs}$  from Eq. (2.22). Differentiating Eq. (2.27) with respect to  $x$  and neglecting higher order terms, we obtain:

$$\{\bar{\mathbf{q}}_{b,x}\} = [\mathbf{C}]^{-1}\{\hat{\mathbf{F}}_b\} \quad (2.28)$$

where,

$$[\hat{\mathbf{F}}_b]^T = [0 \ V_y \ V_z \ T_\omega \ 0]^T \quad (2.28a)$$

where  $T_\omega$  is the Vlasov torsion. In deriving Eq. (2.28), the following relations have been used:

$$[\bar{\mathbf{F}}_{b,x}]^T = [0 \ V_y \ V_z \ T_\omega \ 0]^T \quad (2.29)$$

Considering Equations (2.22) and (2.25) and using Eq. (2.28), we have the relation for  $N_{xs}^r$  as:

$$N_{xs}^r = [F_x \ F_y \ F_z \ F_\omega \ F_\phi]^T [\mathbf{C}]^{-1}\{\hat{\mathbf{F}}_b\} \quad (2.30)$$

This expression can be simplified as:

$$N_{xs}^r = g_y(s)V_y + g_z(s)V_z + g_\omega(s)T_\omega \quad (2.31)$$

where  $g_y$ ,  $g_z$  and  $g_\omega$  are the shear-related warping terms and represent the sectional distribution of shear which result in shear correction coefficients for the section in the respective directions. From the variational equation in Eq. (2.14), we can obtain the force vector  $\{\hat{\mathbf{F}}_b\}$  in terms of strains as:

$$\{\hat{\mathbf{F}}_b\} = [\bar{\mathbf{E}}]^{-1}[\bar{\mathbf{D}}]\{\mathbf{q}_b\} \quad (2.32)$$

where the components in  $[\bar{\mathbf{E}}]$  and  $[\bar{\mathbf{D}}]$  are given in Appendix ((a.2) and (a.3)) and  $\{\mathbf{q}_b\}$  is the generalized displacement vector which is defined as:

$$\{\mathbf{q}_b\} = [U_{,x} \ \gamma_{xy} \ \gamma_{xz} \ \phi_{,x} \ \beta_{y,x} \ \beta_{z,x} \ \phi_{,xx}]^T \quad (2.33)$$

Substituting Eq. (2.30) into Eq. (2.27) and using Eq. (2.28), we obtain:

$$[\bar{\mathbf{F}}_b]^T = [\mathbf{C}]\{\bar{\mathbf{q}}_b\} + [\bar{\mathbf{B}}][\mathbf{C}]^{-1}[\bar{\mathbf{E}}]^{-1}[\bar{\mathbf{D}}]\{\mathbf{q}_b\} \quad (2.34)$$

Combining Equations (2.32) and (2.34) and using the relation for the torque,  $T=T_x+T_\omega$ , we obtain the beam equation as:

$$\{\mathbf{F}_b\} = [\mathbf{K}]\{\mathbf{q}_b\} \quad (2.35)$$

where,

$$[\mathbf{F}_b]^T = [N \ V_y \ V_z \ T \ M_y \ M_z \ M_\omega]^T \quad (2.36)$$

The (7x7) stiffness matrix of Eq. (2.35) represents the beam stiffness matrix at a Timoshenko level of approximation. The nonlinear distribution of the shear strains is

considered in calculating the shear correction factors and the stiffness matrix is expressed in terms of the shear strains at the neutral axis. The stiffness matrix is derived in two stages. First, the (5x5) matrix of Eq. (2.27) consists of two parts: the [C] matrix which is equivalent to an Euler-Bernoulli approximation and the matrix  $\overline{[B]}$  which represents the correction due to the reactive forces. When the effects of shear corrections are not significant, the [C] matrix gives results of good accuracy. In the second step, the reactive shear flow is obtained in terms of the externally applied loads and the associated warpings (Eq. (2.31)). The shear-related warping functions,  $g_x, g_y, g_z$  are obtained in closed form in Eq. (2.31). These shear-related warping terms are used to express the applied forces in terms of the generalized strains (Eq. (2.32)). Combining these relations leads to the (7x7) stiffness matrix (Eq. (2.35)).

### 2.5 Comparison with Other Theories

In order to compare the present theory with other methods, we first consider the (5x5) [C] matrix of Eq. (2.35). This matrix is symmetric and its elements for single-celled cross-section beams are given in Appendix (Eq. (a.1)). In Eq. (a.1), the associated terms containing  $f_i$ 's arise from the redundant part of the shear flow equation in Eq. (2.22) and are only applicable to closed cross-sections. For beams with open cross-sections, these terms in all the elements of the stiffness matrix are equivalent to zero.

Berdichevsky, *et al.* [9] have derived similar expressions for beams of open cross-section. For beams of closed cross-section, they have derived the corresponding (4x4) matrix that neglected the warping restraint effects. They use the plane stress approximation for the constitutive relations. For beams with closed cross-section, they do not include the thickness terms in their analysis. Taking these differences into account, the stiffness matrices derived by Berdichevsky *et al.* are identical to those

obtained in the present paper. Chandra and Chopra [5] have extended the Vlasov theory to composite beams of both open and closed cross-sections using a displacement formulation. For both types of cross-sections, their model is a Timoshenko type theory with the shear correction factor set to unity. The stiffness matrix derived by Chandra and Chopra [5] is of the order (9x9) since they include  $\gamma_{xy,x}$  and  $\gamma_{xz,x}$  as independent degrees of freedom in their formulation, while they are included in the curvatures in the present paper (Eq. (2.4)). In addition, they used the plane strain assumption for the constitutive relations whereas in the present paper, the reduced stiffness terms (Eq. (2.12) are used. After accounting for these factors, the [C] matrix of the present paper agrees with the stiffness terms presented by Chandra and Chopra for both open and closed cross-section blades. In addition, the shear related terms of the present paper agree with the corresponding terms of Ref. 5 if the shear correction factors are set to unity. For composite beams with thin-walled closed cross-sections, the (7x7) matrix of the present paper with the shear correction terms set to unity has a form similar to that used by Rehfield *et al.* [3] who used a stiffness formulation. They used the plane stress assumption for the constitutive relations.

## 3. Examples

In order to bring out the special features of the present formulation, it is instructive to consider some examples where closed-form solutions are available. A solid rectangular beam and an I-beam both having symmetric layup are considered.

### 3.1 Solid Rectangular Section Beam

Consider a composite beam with solid rectangular cross-section with a generally orthotropic layup in which all the fibres are oriented at the same angle  $\theta$  to the beam axis. The width and height of the beam are

$2b$  and  $2h$ , respectively. Such a beam exhibits bending-torsion and extension-shear couplings. The non-zero stiffness elements for this beam are:

$$\begin{aligned}
 K_{11} &= 2b(A_{n\epsilon} + \frac{5}{6} \frac{A_{16}^2}{A_{66}}) \\
 K_{12} &= 2b(\frac{5}{6} A_{16}) \quad , \quad K_{22} = 2b(\frac{5}{6} A_{66}) \\
 K_{33} &= 2bA_{55} \quad , \quad K_{44} = 8bD_{66} \quad (3.1) \\
 K_{45} &= 2bD_{16} \quad , \quad K_{55} = \frac{2h^3}{3} A_{n\epsilon} \\
 K_{66} &= \frac{2b^3}{3} A_{n\epsilon} \quad , \quad K_{77} = \frac{2b^3}{3} D_{11}
 \end{aligned}$$

The elements of the stiffness matrix are the same as those obtained by Chandra and Chopra [5] for a rectangular beam with symmetric lay-up. Their formulation is equivalent to using a shear correction factor of unity instead of (5/6) obtained in the present formulation. It is noteworthy that the shear correction factor affects not only the direct shear stiffness,  $K_{22}$ , but also both the axial stiffness ( $K_{11}$ ) and the coupling stiffness ( $K_{12}$ ).

### 3.2 I-Beam

For an I-beam with width  $2b$  and height  $2h$  having a symmetric lay-up (Fig. 2), the shear stiffness  $K_{33}$  in the vertical direction is identified as:

$$K_{33} = k_z \left( \frac{2h}{A_{\gamma\tau}^w} \right) \quad (3.2)$$

where the superscript  $w$  denotes web of I-beam and  $k_z$  is the shear correction factor which can be written as:

$$k_z = \frac{10(3m+1)^2}{(12+60m+90m^2+15m^2n)} \quad (3.3)$$

with

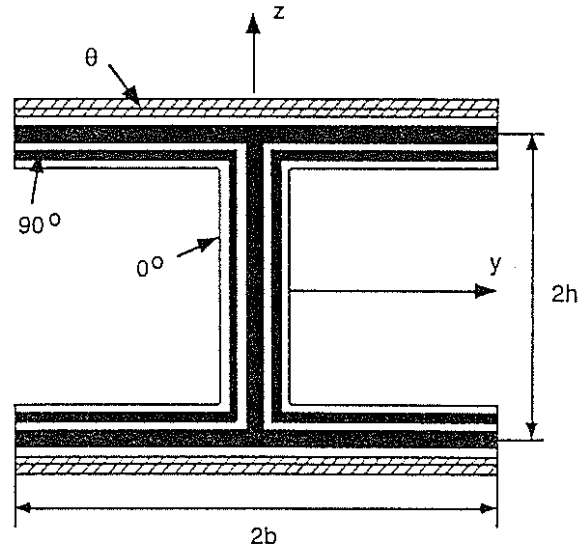


Fig. 2 Layup configurations in a symmetric I-beam.

$$\begin{aligned}
 m &= \frac{b(A_{n\epsilon}^t + A_{n\epsilon}^b)}{hA_{n\epsilon}^w} \\
 n &= \frac{b(A_{\gamma\tau}^t + A_{\gamma\tau}^b)}{hA_{\gamma\tau}^w}
 \end{aligned} \quad (3.3a)$$

where the superscript  $t$  and  $b$  denote the top and bottom flanges of the I-beam. For the case of  $m = 0$ , (i.e., when the flange is absent), the shear correction factor becomes (5/6), which is the same value as for a rectangular beam. It is noted that the shear correction factor given in Eq. (3.3) is different from that given by Cowper [16] for isotropic I-beams and by Banks [17] for orthotropic I-beams, since both Cowper and Banks define the deformations as average values over the cross-section, while in the present paper, these correspond to the neutral axis of the beam.

### 4. Finite Element Formulation

The finite element equations are derived through the application of the stationary potential energy theorem. The potential energy for the beam undergoing extension, flap- and lag-bending, shear, torsion and warping deformation can be expressed as:

$$\Pi = \frac{1}{2} \int_0^L \mathbf{q}_b^T \mathbf{F}_b dx - \frac{1}{2} \int_0^L \mathbf{q}_b^T \mathbf{f}_c dx \quad (4.1)$$

$\mathbf{F}_b$  is the vector of one-dimensional generalized bar forces (Eq. (2.36)),  $\mathbf{q}_b$  is the corresponding deformations (Eq. (2.33)) and  $\mathbf{f}_c$  is the generalized load vector which is defined as:

$$\mathbf{f}_c^T = [n \quad q_y \quad q_z \quad m_y \quad m_z \quad m_\omega \quad t_x] \quad (4.2)$$

The components in  $\mathbf{f}_c$  are generalized load intensities on the beam, derived from the loadings on shell [14]. Inserting Eq. (2.35) into Eq. (4.1) and applying stationary condition,  $\delta\Pi = 0$ , yields

$$\delta\Pi = \int_0^L \mathbf{q}_b^T \mathbf{K}_c \delta\mathbf{q}_b dx - \int_0^L \delta\mathbf{q}_b^T \mathbf{f}_c dx = 0 \quad (4.3)$$

In the finite element formulation, the bending and twist deformations are interpolated using a two-node Hermite shape function to satisfy the  $C^1$  continuity at each extremity of an element. The axial and shear degrees of freedom are interpolated by a four-node Lagrangian shape function and a two-node Lagrangian shape function, respectively. This yields the following set of bar displacements in terms of nodal variables and shape functions over the element.

$$\begin{aligned} U &= \mathbf{H}_u^T \mathbf{q}_u \\ V &= \mathbf{H}_v^T \mathbf{q}_v \\ W &= \mathbf{H}_w^T \mathbf{q}_w \\ \phi &= \mathbf{H}_\phi^T \mathbf{q}_\phi \\ \gamma &= \mathbf{H}_\gamma^T \mathbf{q}_\gamma \end{aligned} \quad (4.4)$$

where the nodal displacement vectors are:

$$\begin{aligned} \mathbf{q}_u^T &= [U_1 \quad U_2 \quad U_3 \quad U_4] \\ \mathbf{q}_v^T &= [V_1 \quad V_1' \quad V_2 \quad V_2'] \\ \mathbf{q}_w^T &= [W_1 \quad W_1' \quad W_2 \quad W_2'] \\ \mathbf{q}_\phi^T &= [\phi_1 \quad \phi_1' \quad \phi_2 \quad \phi_2'] \\ \mathbf{q}_\gamma^T &= [\gamma_{xy_1} \quad \gamma_{xy_2} \quad \gamma_{xz_1} \quad \gamma_{xz_2}] \end{aligned} \quad (4.5)$$

The result of this finite element is a four node, 20 degrees of freedom element that can capture extension, bending, shear, torsion and warping deformations. Inserting these discretized displacements into the potential energy expression and integrating over the beam length results in the following set of finite element beam equations:

$$\mathbf{K}_E \mathbf{q}_E = \mathbf{F}_E \quad (4.6)$$

where  $\mathbf{F}_E$  is an element force vector, and the stiffness matrix,  $\mathbf{K}_E$ , and the generalized displacement vector,  $\mathbf{q}_E$ , are given by:

$$\mathbf{K}_E = \begin{bmatrix} \mathbf{K}_{uu} & \mathbf{K}_{uv} & \mathbf{K}_{uw} & \mathbf{K}_{u\phi} & \mathbf{K}_{u\gamma} \\ & \mathbf{K}_{vv} & \mathbf{K}_{vw} & \mathbf{K}_{v\phi} & \mathbf{K}_{v\gamma} \\ & & \mathbf{K}_{ww} & \mathbf{K}_{w\phi} & \mathbf{K}_{w\gamma} \\ & & & \mathbf{K}_{\phi\phi} & \mathbf{K}_{\phi\gamma} \\ Sym & & & & \mathbf{K}_{\gamma\gamma} \end{bmatrix} \quad (4.6a)$$

$$\mathbf{q}_E^T = [\mathbf{q}_u^T \quad \mathbf{q}_v^T \quad \mathbf{q}_w^T \quad \mathbf{q}_\phi^T \quad \mathbf{q}_\gamma^T] \quad (4.6b)$$

The components in the element stiffness matrix represent the magnitude of direct and coupling stiffnesses.  $\mathbf{K}_{uu}$  is direct extension stiffness,  $\mathbf{K}_{uv}$  is coupling stiffness between extension and lag bending motions. The other terms in the stiffness equations can be defined in a similar manner. Depending on particular composite layups used in the beam structure, these coupling stiffnesses play a significant role as discussed in Ref. 1. The finite element stiffness matrix in Eq. (4.6a) is similar to that of Floros and Smith [18] except the shear coupling terms.

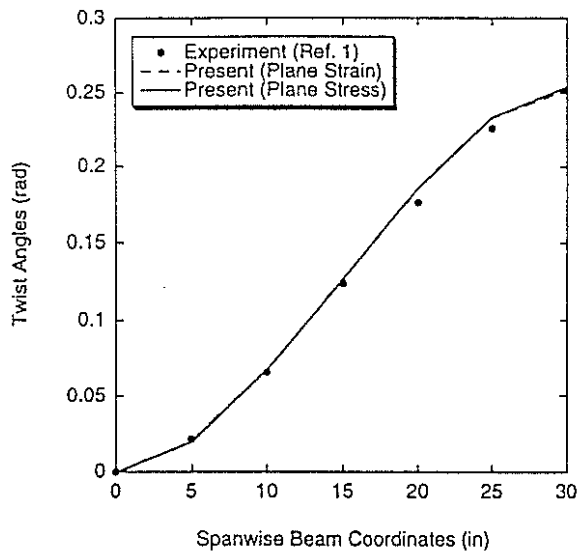


Fig. 3 Variation of twist in a symmetric  $[(0/90)_2]_s$  I-beam under unit tip torque.

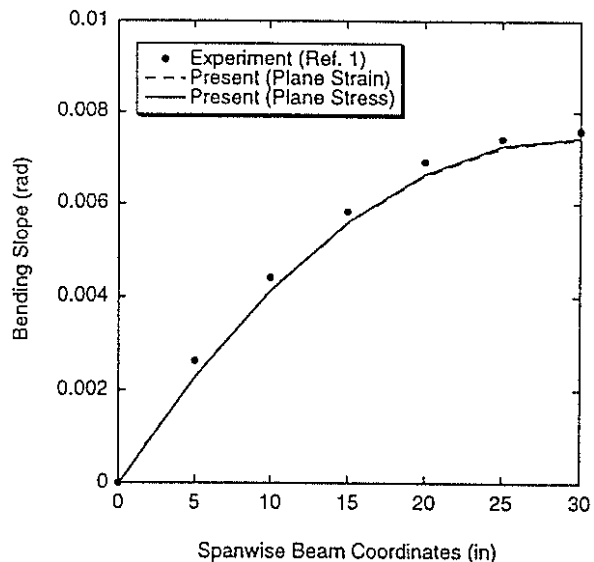


Fig. 4 Variation of bending slope in a symmetric  $[(0/90)_2]_s$  I-beam under unit tip bending load.

## 5. Results and Discussion

Numerical predictions for symmetric composite I-beams undergoing different types of loading are evaluated to validate the current approach against experimental data and other existing analytic beam results. The I-beams used in the comparison study were tested by Chandra and Chopra [5] and the mechanical material properties are presented in Table 1. The beam has a length of 30 in. with 1 in. x 0.5 in. section. Figure 2 shows the details of the layups for the I-beam. The I-section has a symmetric configuration with respect to the beam axis:  $[(0/90)_2]_s$  for web and  $[(0/90)_3/\theta_2]$  for flanges.

Figure 3 represents the results for the twist distribution of a cantilevered I-beam with  $[(0/90)_2]_s$  layups in web and  $[(0/90)_2]_s$  layups in flanges. The beam is subjected to a unit tip torque. The beam is clamped at the root with warping restrained both at the root and loading tip. The current predictions were obtained by using 12 beam finite elements for ease of comparison with experimental test data performed by Chandra and Chopra [5]. Both the results of plane strain and plane stress cases are

presented in this plot. Very good correlation between the current results and the test data is seen over the entire beam length. The results for the variation of bending slope for this uncoupled configuration undergoing unit tip bending load (vertical shear load) is presented in Fig. 4. Though not noticeable, the plane stress approximation shows a slightly better correlation than the plane strain approximation. This slight difference between the two cases is due to the inclusion of  $A_{12}$ ,  $A_{22}$  and  $D_{22}$  for the cross ply configuration beams. The correlation is also seen to be good.

Results for bending-torsion coupled I-beams are presented in Figs. 5 to 7. Figure 5 shows the comparison results for the twist distribution along the beam span subjected to unit tip torque. The beam considered had flange layups of  $[(0/90)_3/30_2]$  and a web layup of  $[(0/90)_2]_s$ . The present finite element results are compared with experimental test data of Ref. 5 and with the results of Berdichevski *et al.* [9] which are reproduced here for the comparison. The present results in Fig. 5 are categorized into three parts according to the approximations made in the beam kinematic and/or constitutive relations: (a) displacement-based approach with plane strain assumption which is similar to Chandra and

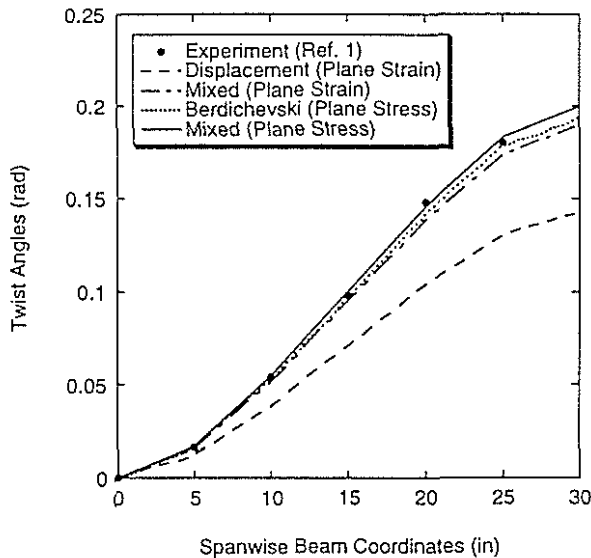


Fig. 5 Variation of twist in a symmetric  $[(0/90)_3/30_2]$  I-beam under unit tip torque.

Chopra [5]; (b) mixed approach with plane strain assumption; (c) mixed approach with plane stress assumption. The term, *mixed*, is used here because the current approach uses both the displacement and stiffness formulation. As can be seen in this plot, the current predictions with plane stress assumptions present the best correlation with experimental data. This fact is due to the additional flexibility introduced by plane stress assumption together with the mixed formulation used in the beam kinematics. It is noted that the results of the mixed formulation with plane strain assumption are comparable to those of Bedichevski *et al.* [9].

Figure 6 shows the variation of bending slope along the beam span for the beam loaded with a unit tip bending load. The flange layup for this case is  $[(0/90)_3/15_2]$  with web layup of  $[(0/90)_2]_s$ . In this figure, all the four cases are listed together for comparison with experimental test data. The analytical results slightly underpredict the bending deformations in comparison with test data, but, as a whole, the correlation is good. Figure 7 presents the distribution of bending induced twist along the beam span for the 15 deg. I-beam configuration. For

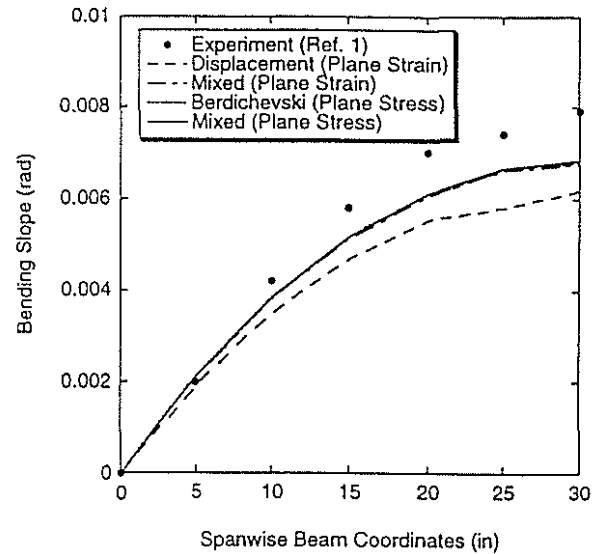


Fig. 6 Variation of bending slope in a symmetric  $[(0/90)_3/15_2]$  I-beam under unit tip bending load.

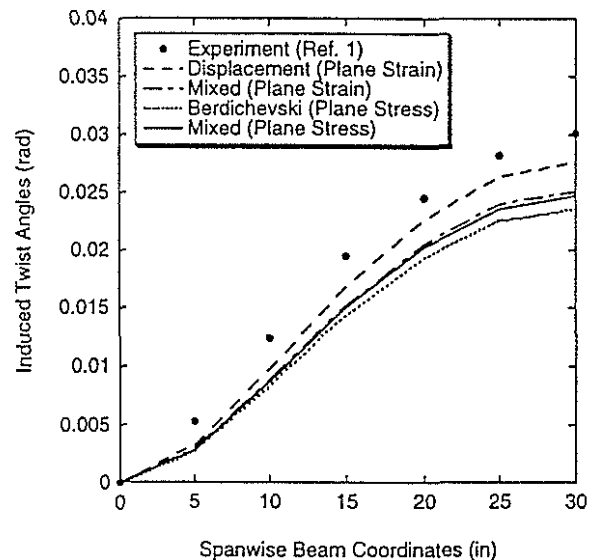


Fig. 7 Variation of bending induced twist in a symmetric  $[(0/90)_3/15_2]$  I-beam under unit tip bending load.

this particular case, the displacement solutions with plane strain assumption show an excellent correlation with experimental test data. Generally, the other predictions are in a good agreement with test data, especially with plane strain assumptions.

## 6. Conclusions

A structural model has been presented for the analysis of composite blades with elastic couplings. The model includes the influence of the thickness of the wall and accounts for the non-uniform distribution of the shear strains due to bending and torsion. Beams of open and closed cross-section are modeled in a unified approach which is based on a semi-complementary energy functional and combines the displacement formulation with the flexibility formulation. The bending and torsion warpings are derived in a closed form and all the terms in the warpings are retained. Comparison with other theories shows that the Euler-Bernoulli formulation which is a subset of the present formulation is easy to apply and has more features such as inclusion of thickness effects than those available in other theories. Closed form solutions for bending-torsion coupled beam of solid rectangular cross section and I-beam show that the influence of the shear correction affects not only the direct shear term but also the axial and coupling terms. Comparison of results for bending-torsion coupled I-beams shows that the present method gives results which have a good agreement with experiments.

## Acknowledgments

This work was supported by the National Rotorcraft Technology Center under Grant No. NCC 2944. Technical monitor is Dr. Yung Yu.

## References

1. Jung, S. N., Nagaraj, V. T. and Chopra, I., "Assessment of Composite Rotor Blade Modeling Techniques," *AHS International Meeting on Advanced Rotorcraft Technology and Disaster Relief*, Gifu, Japan, April 21-23, 1998.
2. Rehfield, L. W., "Design Analysis Methodology for Composite Rotor Blades," *7th DoD/NASA Conference on Fibrous Composites in Structural Design*, Denver, June 17-20, 1985.
3. Rehfield, L. W., Atilgan, A. R., and Hodges, D. H., "Nonclassical Behavior of Thin-Walled Composite Beams with Closed Cross Sections," *Journal of the American Helicopter Society*, Vol. 35, No. 2, 1990, pp. 42-51.
4. Smith, E. C. and Chopra, I., "Formulation and Evaluation of an Analytical Model for Composite Box-Beams," *Journal of the American Helicopter Society*, Vol. 36, No. 3, July 1991, pp. 23-35.
5. Chandra, R. and Chopra, I., "Experimental and Theoretical Analysis of Composite I-Beams with Elastic Couplings," *AIAA Journal*, Vol. 29, No. 12, Dec. 1991, pp. 2197-2206.
6. Mansfield, E. H. and Sobey, A. J., "The Fiber Composite Helicopter Blade, Part I: Stiffness Properties, part II: Prospects for Aeroelastic Tailoring," *Aeronautical Quarterly*, Vol. 30, 1979.
7. Libove, C., "Stress and Rate of Twist in Single-Cell Thin-Walled Beams with Anisotropic Walls," *AIAA Journal*, Vol. 26, No. 9, 1988, pp. 1107-1118.
8. Johnson, E. R., Vasiliev, V. V. and Vasiliev, D. V., "Anisotropic Thin-Walled Beams with Closed Cross-Sectional Contours," *Proceedings of the AIAA/ASME/ASCE/AHS/ASC 39th Structures, Structural Dynamics, and Materials Conference*, AIAA 98-1761, 1998, pp. 500-508.
9. Berdichevsky, V. L., Armanios, E., and Badir, A., "Theory of Anisotropic Thin-Walled Closed-Cross-Section Beams," *Composites Engineering*, Vol. 2, Nos. 5-7, 1992, pp. 411-432.
10. Suresh, J. K. and Nagaraj, V. T., "Higher-Order Shear Deformation Theory for Thin-Walled Composite Beams," *Journal of Aircraft*, Vol. 33, No. 5, 1996, pp. 978-986.

11. Hodges, D. H., Atilgan, A. R., Cesnik, C. E. S. and Fulton, M. V., "On a Simplified Strain Energy Function for Geometrically Nonlinear Behavior of Anisotropic Beams," *Composites Engineering*, Vol. 2, Nos. 5-7, 1992, pp. 513-526.
12. Kraus, H., *Thin Elastic Shells*, John Wiley & Sons, 1967.
13. Jones, R. M., *Mechanics of Composite Materials*, Ch. 5, 1975.
14. Murakami, H., Reissner, E. and Yamakawa, J., "Anisotropic Beam Theories with Shear Deformation," *Journal of Applied Mechanics*, Vol. 63, Sept. 1996, pp. 660-668.
15. Gjelsvik, A., *The Theory of Thin Walled Bars*, John Wiley & Sons, Inc., 1981.
16. Cowper, G. R., "The Shear Coefficient in Timoshenko's Beam Theory," *Journal of Applied Mechanics*, June 1966, pp. 335-340.
17. Banks, L. C., "Shear Coefficients for Thin-Walled Composite Beams," *Composite Structures*, Vol. 8, No. 1, 1987, pp. 47-61.
18. Floros, M. W. and Smith, E. C., "Finite Element Modeling of Open-Section Composite Beams with Warping Restraint Effects," *AIAA Journal*, Vol. 35, No. 8, 1997, pp. 1341-1347.

### Appendix

The elements of matrix [C] in Eq. (2.27) can be identified as:

$$\begin{aligned}
 C_{11} &= \int_C A_{ne} ds + f_x^2 \int_C A_{\gamma r} ds \\
 C_{12} &= \int_C (A_{ne} z - A_{n\kappa} y_{,s}) ds + f_x f_z \int_C A_{\gamma r} ds \\
 C_{13} &= \int_C (A_{ne} y + A_{n\kappa} z_{,s}) ds + f_x f_y \int_C A_{\gamma r} ds \\
 C_{14} &= \int_C (-A_{ne} \bar{\omega} + A_{n\kappa} q) ds + f_x f_\omega \int_C A_{\gamma r} ds \\
 C_{15} &= \int_C 2A_{n\phi} z ds + f_x f_\phi \int_C A_{\gamma r} ds \\
 C_{22} &= \int_C (A_{ne} z^2 - 2A_{n\kappa} z y_{,s} + A_{m\kappa} y_{,s}^2) ds \\
 &\quad + f_z^2 \int_C A_{\gamma r} ds \\
 C_{23} &= \int_C (A_{ne} y z + A_{n\kappa} (z z_{,s} - y y_{,s}) \\
 &\quad - A_{m\kappa} y_{,s} z_{,s}) ds + f_z f_y \int_C A_{\gamma r} ds \\
 C_{24} &= \int_C ((-A_{ne} z + A_{n\kappa} y_{,s}) \bar{\omega} + (A_{n\kappa} z \\
 &\quad - A_{m\kappa} y_{,s}) q) ds + f_z f_\omega \int_C A_{\gamma r} ds \quad (a.1) \\
 C_{25} &= \int_C 2(-A_{n\phi} z + A_{m\phi} y_{,s}) ds \\
 &\quad + f_z f_\phi \int_C A_{\gamma r} ds \\
 C_{33} &= \int_C (A_{ne} y^2 + 2A_{n\kappa} y z_{,s} + A_{m\kappa} z_{,s}^2) ds \\
 &\quad + f_y^2 \int_C A_{\gamma r} ds \\
 C_{34} &= \int_C ((-A_{ne} y - A_{n\kappa} z_{,s}) \bar{\omega} + (A_{n\kappa} y \\
 &\quad + A_{m\kappa} z_{,s}) q) ds + f_y f_\omega \int_C A_{\gamma r} ds \\
 C_{35} &= \int_C 2(-A_{n\phi} y + A_{m\phi} z_{,s}) ds \\
 &\quad + f_y f_\phi \int_C A_{\gamma r} ds \\
 C_{44} &= \int_C (A_{ne} \bar{\omega}^2 - 2A_{n\kappa} q \bar{\omega} + A_{m\kappa} q^2) ds \\
 &\quad + f_\omega^2 \int_C A_{\gamma r} ds \\
 C_{45} &= \int_C 2(A_{n\phi} \bar{\omega} - A_{m\phi} q) ds + f_\omega f_\phi \int_C A_{\gamma r} ds \\
 C_{55} &= \int_C 4A_{\phi\phi} ds + f_\phi^2 \int_C A_{\gamma r} ds
 \end{aligned}$$

The elements of matrices [ $\bar{\mathbf{E}}$ ] and [ $\bar{\mathbf{D}}$ ] in Eq. (2.32) are obtained respectively as:

$$\begin{aligned}
\bar{E}_{11} &= \int_C A_{\gamma\tau} g_y^2 ds \\
\bar{E}_{12} &= \int_C A_{\gamma\tau} g_y g_z ds \\
\bar{E}_{13} &= \int_C A_{\gamma\tau} g_y g_\omega ds \\
\bar{E}_{22} &= \int_C A_{\gamma\tau} g_z^2 ds \\
\bar{E}_{23} &= \int_C A_{\gamma\tau} g_z g_\omega ds \\
\bar{E}_{33} &= \int_C A_{\gamma\tau} g_\omega^2 ds
\end{aligned}
\tag{a.2}$$

The expressions for  $\bar{D}_{2i}$  and  $\bar{D}_{3i}$  ( $i = 1, 7$ ) are same as  $\bar{D}_{1i}$  except that  $g_y$  is replaced

$$\begin{aligned}
\bar{D}_{11} &= \int_C g_y (A_{n\tau} - A_{\gamma\tau} f_x) ds \\
\bar{D}_{12} &= \int_C g_y y_{,s} ds \\
\bar{D}_{13} &= \int_C g_y z_{,s} ds \\
\bar{D}_{14} &= \int_C g_y (-2A_{\phi\tau} - A_{\gamma\tau} f_\phi) ds \\
\bar{D}_{15} &= \int_C g_y (A_{n\tau} z - A_{m\tau} y_{,s} - A_{\gamma\tau} f_z) ds \\
\bar{D}_{16} &= \int_C g_y (A_{n\tau} y + A_{m\tau} z_{,s} - A_{\gamma\tau} f_y) ds \\
\bar{D}_{17} &= \int_C g_y (A_{n\tau} \bar{\omega} + A_{m\tau} q - A_{\gamma\tau} f_\omega) ds
\end{aligned}
\tag{a.3}$$

by  $g_z$  and  $g_\omega$ , respectively. Note that  $[\bar{\mathbf{E}}]$  is symmetric whereas  $[\bar{\mathbf{D}}]$  is asymmetric.